PROCEEDINGS of the
23rd International Congress on Acoustics

9 to 13 September 2019 in Aachen, Germany

Predicting cooling fan noise by numerical conditions using compressible Large Eddy Simulation

Kimihisa KANEKO[1]; Tsutomu YAMAMOTO[2]

[1,2] Fuji Electric Co., Ltd., Japan

ABSTRACT

This paper describes predicting motor fan noise using direct computational aeroacoustics (direct CAA) methods. In the direct CAA method, both turbulent flow and acoustic phenomenon are solved at the same time with compressible Navier-Stokes equation. Large Eddy Simulation is applied for solving turbulent flow. Direct CAA can predict aeroacoustics without any assumption model such as a rotating fan. Therefore high accuracy results can be obtained. On the other hand, much computational time are required. For the reason, it is required to reduce the computational time for developing new product with short time period.

We investigated the relation between the computational time and their accuracy. Specifically, computational time step can be reduced computational time, and accuracy were investigated in terms of pressure fluctuation on the sound source side and acoustic effect on the sound receiver side in this study.

Keywords: Aeroacoustics, Large Eddy Simulation, Compressible turbulence flow

1. INTRODUCTION

Recent trends of electric equipment miniaturization have caused an increase in the heat generation density and an accompanying need to increase airflow to enable cooling. Therefore, aerodynamic noise from fans has become a dominant source of noise in air-cooled electrical equipment. Fan noise is known to be influenced by the fan operating point and the fan's surrounding structures(1, 2, 3). Predicting the noise level when designing electronic equipment incorporating a fan is important, as is understanding aerodynamic noise phenomena under various practical conditions. Nevertheless, it is difficult to characterize the sound source without considering the structure of the electric components and the fan. The authors' previous study specifically addressed fan noise using a non-axisymmetric structure to elucidate the noise-generation mechanism related to the electronic equipment(4).Either the hybrid computational aeroacoustics (CAA) method or the direct CAA method can be used to conduct a numerical analysis of aerodynamic noise.

The hybrid CAA method uses incompressible Navier-Stokes equations to compute turbulent flow and the acoustic wave separately. Furthermore, turbulent fluctuation, which is the source of acoustic propagation, is obtainable using several turbulent models: LES, Detached Eddy Simulation (DES), Unsteady Reynolds Averaged Navier-Stokes (U-RANS), and acoustic propagation are obtainable using Lighthill's acoustic analogy(5). The effectiveness of using the hybrid CAA method for analyzing aerodynamic noise from a centrifugal fan(6, 7, 8) and an axial flow fan(9, 10) have been described in earlier reports. Furthermore, predicting aeroacoustics noise of complex geometry such as electronic devices have been investigated with several U-RANS based turbulent model and acoustics(11).

The direct CAA method uses compressible Navier-Stokes equations to compute both the turbulent flow and the acoustic wave. High-order numerical schemes must be used to resolve turbulent and acoustic fluctuations(12). Interaction between fluid and acoustics have been investigated using high-order numerical schemes with two-dimensional cavity flow(13, 14).

The authors' previous study addressed axial fan noise prediction with an obstacle effect using direct CAA method(15). In terms of sound pressure level, our direct CAA model using second order

[1] kaneko-kimihisa@fujielectric.com

numerical schemes have been obtained good agreement with the experimental result. As described herein, we investigated the possibility of the direct CAA method to develop low noise products. Especially, the sound pressure level (SPL) and pressure fluctuation with the direct CAA model were verified with experiments for a simplified motor structure.

The authors' previous study using direct CAA method for predicting motor fan noise, the simulation model have been obtained good agreement with the experimental result(18). Specifically, the sound pressure level (SPL) at the observation location and pressure fluctuation in the sound source field. For conducting the practical application using direct CAA, computational time should be reduced. In this study, we investigate the predicting SPL accuracy and their computational time depending on the time step.

2. EXPERIMENTAL METHOD

2.1 Experimental structure for verification of direct CAA model

Figure 1 portrays the experimental structure for functional verification. This structure comprises five parts, which is a frame, cooling fin, fan, a fan driving motor, and a cover, to verify aeroacoustics phenomena. Cooling fins are arranged radially on the frame surface. The fan, which is driven by the fan driving motor, is set at the end of the frame. The fan can be used bi-directionally.

The cover is arranged for flow path and safety purpose. Air flows from outside of the cover through the air intake. Air pushed up by the rotating fan flows past the cooling fins. Experimental conditions are presented in Table 1. The fan rotated between 1000 rpm and 2000 rpm. The typical rotating fan speed of 1780 rpm is defined for comparison in this study.

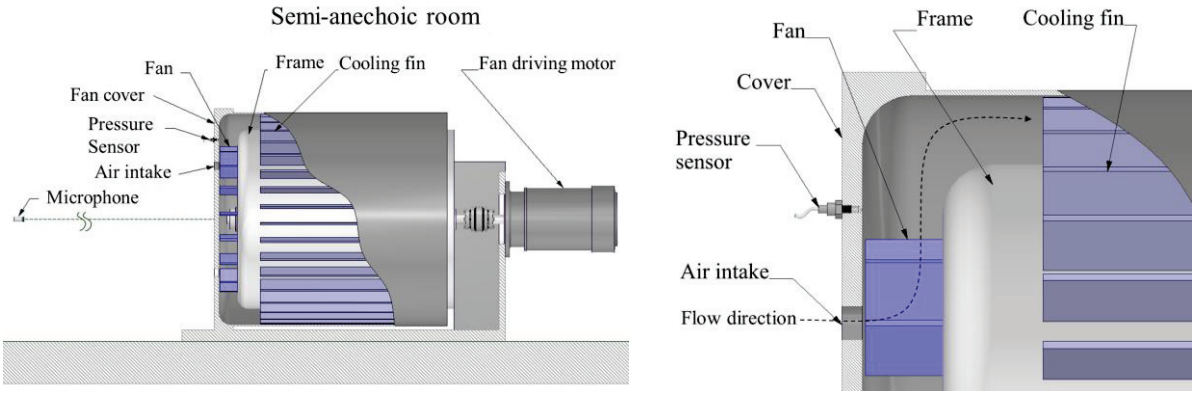

(a)Validation structure (b)Enlargement view

Figure 1 – This is a caption for the figure

Table 1 – Experimental setup

Parameter	Value
Fan diameter D, mm	0.384
Fan blade number Z	17
Rotational speed N, rpm	1780
Blade tip speed u_A, m/s	35.7
Re ($=u_A D/\nu$)	9×10^5
Ma ($=u_A/c_0$)	0.1

2.2 Measurement of the pressure fluctuation and sound pressure level

Sound pressure level measurements and hydraulic pressure fluctuation measurements of the sound source side were taken to verify the numerical simulation results. Pressure fluctuation, which acts on the solid surface, is measured downstream of the fan. The pressure sensor was placed at the fan cover via the pressure hole (1mm) with a recessed mounting to obtain the exact measurement position, as shown in Figure 1(b). However, using this method, the well-known Helmholtz resonance effect occurs.

Therefore, to avoid the Helmholtz resonance in the observation frequency range, the gap dimension was defined. For analysis of the pressure fluctuation in the frequency domain, the pressure signals were measured for 500 s. Subsequently, the Hanning window and overlap factor 0.5 for each segment were used to obtain the power spectra densities. The SPL was measured using a microphone placed at the rotational fan axis height and 1 m distant from the fan cover in the semi-anechoic room. The observation frequency range was as high as 2500 Hz. However, the frequency was as high as 5000 Hz to elucidate the PSD and SPL trend.

3. NUMERICAL SIMULATION METHOD

3.1 Governing Equation

For predicting aeroacoustic noise, the compressible Navier-Stokes equation and energy equation are considered. The LES turbulence model is used to solve the turbulent flow. Moreover, the Dynamic Smagorinsky Model is used as a sub-grid scale model. A Finite Volume Method (FVM) was used to solve the Navier-Stokes equations with the commercial CFD code star-ccm+.

For spatial discretization of the convective term, Bounded Central Differencing (BCD) scheme used for obtaining a stable solution for LES. BCD is based on the Normalized Variable Diagram (NVD) approach. BCD can provide good accuracy and robustness compared with the second-order upwind scheme(16). For temporal discretization, second order implicit Euler method was used.

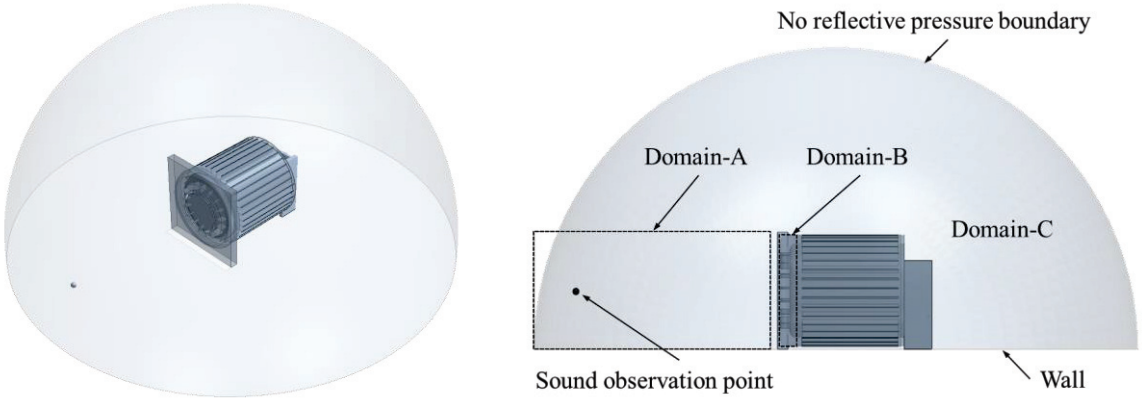

(a)Isometric view (b)Side view

Figure 2 – Computational domain

3.2 Computational grid

Computational grid size defined depending on the dominant physical phenomena, turbulent flow, or sound wave. Fine grid is required to solve the turbulent flow compare to the sound wave propagation. A defined computational grid is shown in Figure 3. The grid size controlled divided into three domains, which is indicated in Figure 2(b). Domain-A: sound wave propagation is dominant. The sound propagates from the motor fan cover to the microphone, which was located 1m distance. The grid size was defined based on the point per wave (PPW). Domain-B: turbulent flow is dominant. The fine grid was made in this area for solving turbulent eddy by LES. The grid size was defined based on the observation frequency range and Reynolds number. Domain-C: the other area of domain A and B. The influence of the observation point assumes small. We made a coarse grid to stable numerical computation.

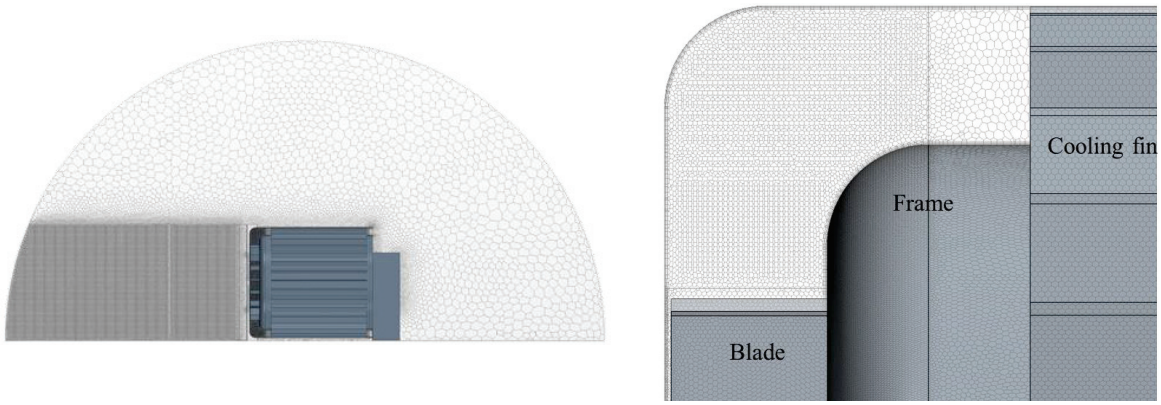

(a)Side view (b) Enlarged view around rotating fan

Figure 3 – Computational grid

3.3 Time step

For evaluating numerical time step dependency on the accuracy of SPL prediction dimensionless value was defined as follows equations. Courant number (CFL), acoustics wave courant number (WCFL) and PPW were used.

$$CFL = \frac{u_{A,B} \cdot dt}{\Delta x} \tag{1}$$

$$WCFL = \frac{c_0 \cdot dt}{\Delta x} \tag{2}$$

$$PPW = \frac{c_0}{f \cdot \Delta x} \tag{3}$$

Therein, $u_{A,B}$ represent typical velocity and subscript indicates domain name. c_0 is acoustic velocity, dt is time step, Δx is grid size, f is maximum frequency range for observation, in this study f = 2500 Hz.

Our defined time step related to the CFL, WCFL and PPW are shown in Table 2. For obtaining the high accuracy result, courant number should be controlled under 1.0 in generally, and PPW is above 10.0 (18). CFL and PPW is sufficient value for all time step and domains. However, in the previous study result, which was defined time step dt = 10 μs, the predicted SPL spectra was in good agreement with experiment. For reducing computational time, time step dependency was evaluated as the base condition is 10 μs.

Table 2 – Defined CFL, WCFL and PPW

Domain	Parameter	Time step [μs]		
		10	15	25
A	CFL[-]	0.010	0.014	0.026
	WCFL[-]	0.34	0.51	0.85
	PPW[-]		15	
B	CFL[-]	0.35	0.5	0.9
	WCFL[-]	3.4	5.1	8.5
	PPW[-]		150	

4. RESULTS AND DISCUSSION

4.1 Turbulent flow

The velocity and averaged pressure distribution are shown in Figure 4. The peak velocity appears downstream of the rotating fan. The flow is circulated counterclockwise by the fan rotation; after it bends 90 deg, it flows between the each cooling fins. Averaged pressure fluctuation indicated as root mean square is shown in Figure 5. High-pressure fluctuation occurs between the leading edge of the blade and downstream of it. Especially, pressure fluctuation increased at the leading edge of the blade, and fan base plate between the blades. The leading edge of the blade, which is close to the intake, is influenced at least eight times by the intake fluctuation per rotation. The fan base plate, which is between the blades, influences the separation flow of the suction side blade.

For analysis of the turbulent flow, the instantaneous second invariant of the velocity gradient tensor, called the Q-criterion, is shown in Figure 6. The Q-criterion indicates and iso-surface colored with velocity magnitude. The Q-criterion is distributed around the rotating fan and downstream of it. A large-scale voritical structure is apparent at the leading edge side of the blade because secondary flow occurs by the separation and leakage flow of the blade. A small-scale voritical structure is distributed near the curved motor frame surface caused by separation flow with a swirl flow.

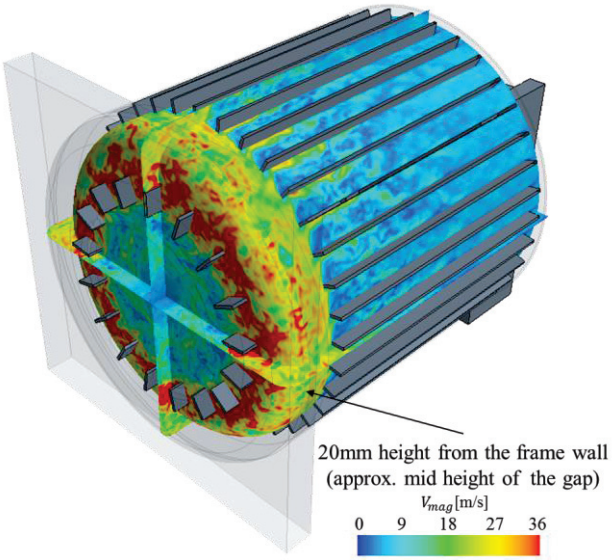

Figure 4 – Velocity distribution (Instantaneous)

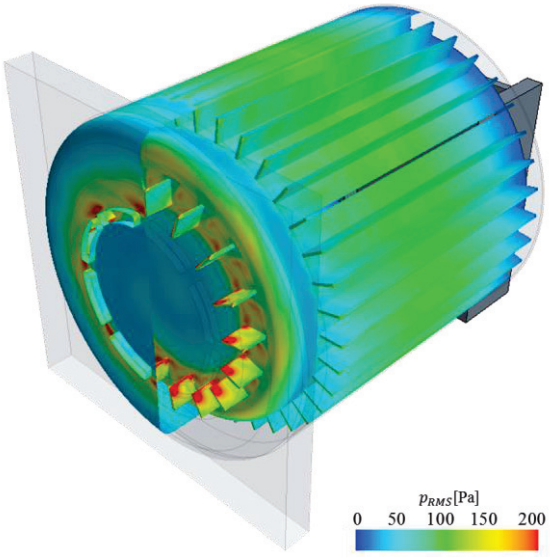

Figure 5 – Pressure distribution (RMS)

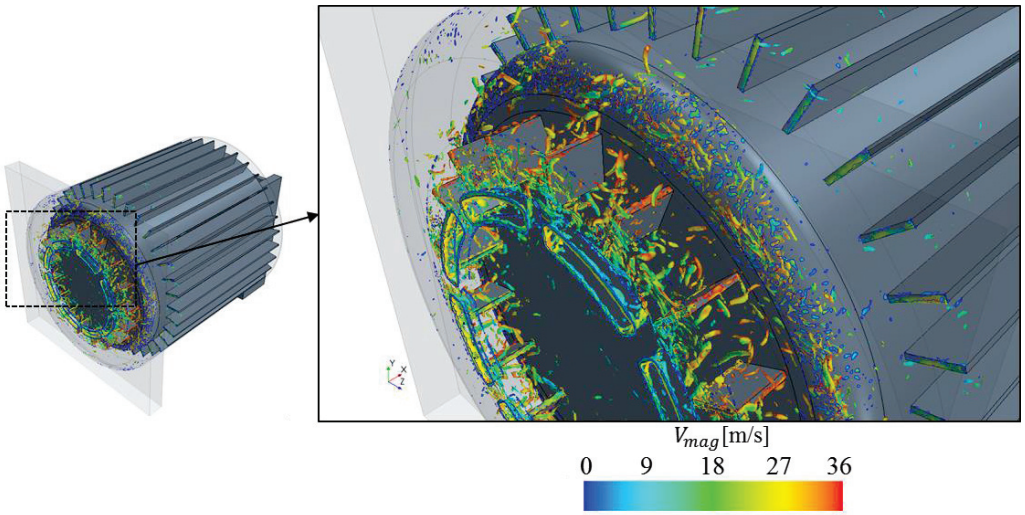

Figure 6 – Q-Criterion distribution colored with velocity ($Q = 1.5 \times 10^7/s^2$)

4.2 Pressure fluctuation in the sound source

For verification of the pressure fluctuation, the computed result and the measured result are compared with power spectra density (PSD), which are shown in Figure 7. Predicted pressure fluctuation PSD results are in good agreement with the measured results up to 2500 Hz of our observation range. A computed PSD trend above the 2500 Hz range is slightly decreasing because the computational grid resolution of LES is insufficient. Pressure fluctuation consists of the dominant frequency and broadband frequency. The dominant frequency is blade passing frequency (BPF), which is based on the blade number and fan rotating frequency. Predicted pressure fluctuation can be solved BPF. The broadband frequency is the influence of turbulent flow. Pressure fluctuation decays above approximately 500 Hz. The trend of their decay is proportional to the frequency of multiplied by -7/3. Pressure fluctuation in the inertial subrange of turbulent flow shown as the following equation(17).

$$p(k) = k^{-7/3} \tag{4}$$

In that equation, k expresses a wave number, which is related to the unsteady turbulent flow frequency. As for various time step, the trend of pressure fluctuation PSD and their value are obtained close to measurement result. However, it was found increasing the time step, decreasing the PSD at high frequency range.

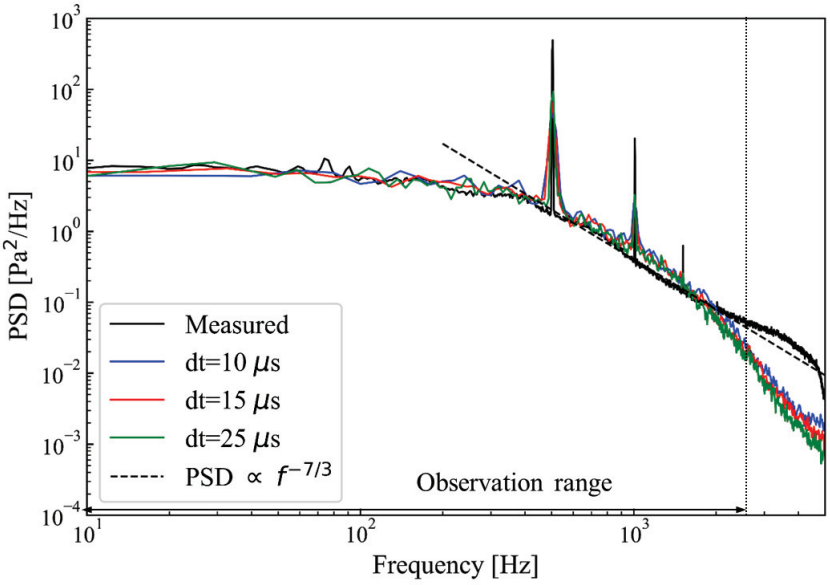

Figure 7 – Pressure fluctuation PSD at each time step

4.3 Sound pressure level

The SPL spectra at the observation point are shown in Figure 8. The SPL includes BPF, broadband noise which cased turbulent flow, and acoustic mode which caused geometry. Predicted SPL with $dt = 10\ \mu s$ was in good agreement with the experimental result. The trend decay of SPL was influenced by the computational time step. As the time step increases, the SPL decay increases. Decayed the SPL spectra much lower frequency compare to the pressure fluctuation. As the frequency is higher, the propagated pressure wave number per time step is increased. Therefore, a high-frequency pressure wave is influenced numerical dissipation compare to the low-frequency. For verification of the SPL decay, sinusoidal frequency pressure source p_{bc}, which shows the following equation, defined inside of the fan cover, which assumed sound noise by the rotating fan.

$$p_{bc}(t) = p_{amp} \sin(2\pi f t) \tag{5}$$

Therein, t is time, p_{amp} is the amplitude of source pressure, f (= 500 Hz, 2500 Hz) is frequency.

Dimensionless pressure, p/p_{amp}, shows in Figure 9. It was confirmed that the propagated pressure decays at high-frequency was affected by the time step compared to the low-frequency with simplified pressure source conditions.

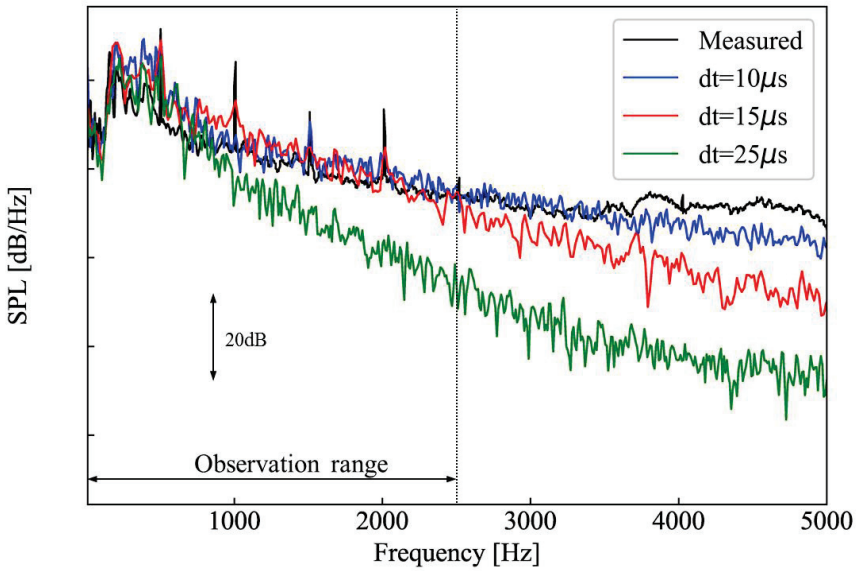

Figure 8– SPL at observation point at each time step

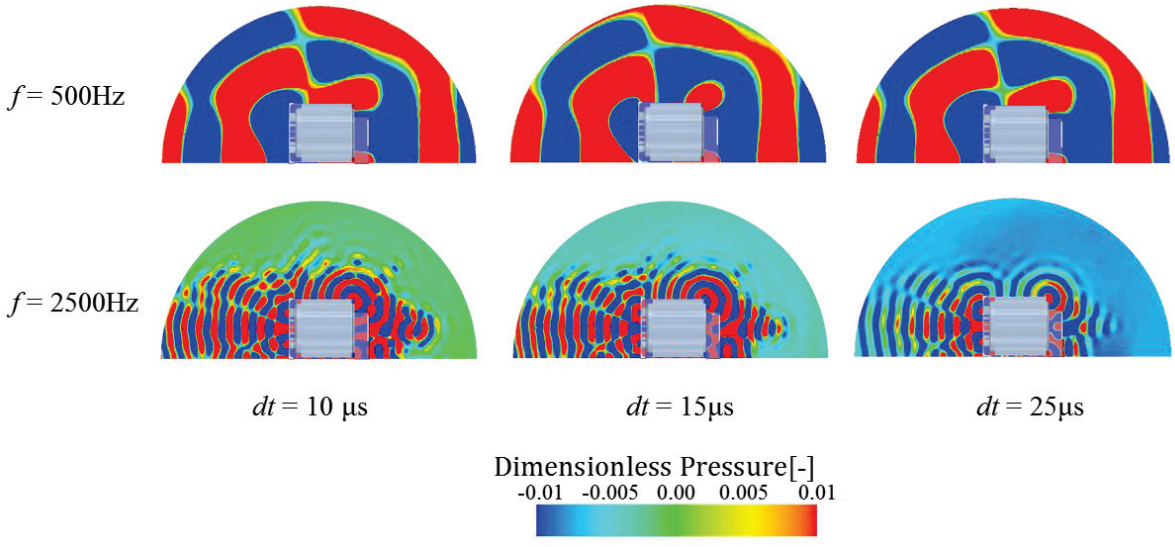

Figure 9 – Dimensionless pressure distribution at each time step and frequency (Instantaneous)

5. CONCLUSIONS

The Direct CAA method applies to predict aeroacoustics noise to develop low noise products. This method can predict sound propagation and turbulent flow simultaneously. On the other hand, direct CAA method is required much computational time compared to the hybrid CAA method, since small time step is needed.

For developing stage of products by using direct CAA method, short computational time and accuracy are required. Therefore, we investigated the time step dependency for accuracy. From our results, we conclude as follows.

(1) Predicted pressure fluctuation PSD and SPL spectra are in good agreement with the experimental result.
(2) Predicted the PSD is in good agreement, not only the BPF but also the trend of PSD decay in the turbulent inertial region corresponds to the experiment.
(3) The computational time step for predicting SPL is more influenced compare to predicting PSD.

REFERENCES

1. Reese H, Carolus T. Axial fan noise: towards sound prediction based on numerical unsteady flow data - a case study. Acoustics 08, Paris; June 29-July 4 2008. p. 4069–4074.
2. Kawaguchi K, Okui K, Kuwaumi M. Effects of turbulence of inlet flow on performance of compact axial flow fan. Turbomachinery Vol.35 No.8 2007. p. 32–40.
3. Fukue, T. et al. The effects of electronic enclosure inlet on p-q curves of in-stalled axial cooling fans. J. JSME Vol.75 No.755 2009. p. 873–880.
4. Kaneko K, Yamamoto T, Kato C. Aerodynamic noise simulation of axial flow fan with non-axisymmetric structure for power electronics equipment. The 13th Asian International Conference on Fluid Machinery, Tokyo, September 7-10, 2015.
5. Lighthill J. On sound generated aerodynamically I. general theory, Proceedings of the Royal Society of London. Series A. Mathematical and Sciences Vol.211 No.1107 1952. p. 564–586.
6. Caro S S, Robert, I, J, Nishino Y. Presentation of a CAA formulation based on Lighthill's analogy for fan noise.. Fan Noise 2007, Lyon, September 17-19, 2007. p. 7–19.
7. Guo Y, Kato C, Yamade Y, Ohta Y, Iwase T and Takayama R. Computation of noise from internal flow in a centrifugal fan., Seisan Kenkyu Vol.66 No.1 2014. p. 27–31.
8. Iwase T, Sato, Daiwa, Obara, Hideshi, Yoneyama, Hiroyasu and Kishitani, Tetsushi. Prediction noise for centrifugal fan of air-conditioner. FAN2015; Lyon, April 15-17, 2015.
9. Takayama R, Kato C. Numerical prediction of aerodynamic noise radiated from propeller fan. Seisan Kenyu Vol.63 No.1 2011. p. 61–64.
10. Bianchi S, Borello D, Corsini A, Rispoli F, Sheard, Anthony G. Large-eddy simulation of the aerodynamic and aeroacoustic performance of a ventilation fan. Advances in Acoustics and Vibration Vol.2013.
11. Munsterjohann S, Grabinger J,Becker S,Kaltenbacher M. CAA of an Air-Cooling System for Electronic Devices. Adv. in Acoustics and Vibration, Vol.2016 Article ID 4785389
12. K.Lele, S. Compact finite difference schemes with spectral-like resolution. Journal of Computational Physics Vol.103 No.1 1992. p. 16–42.
13. Gloerfelt X, Bailly C, Juve D. Direct computation of the noise radiated by a subsonic cavity flow and application of integral methods. Journal of Sound and Vibration Vol.266 No.1 2003. p. 119–146.
14. Yokoyama H, Kato C. Fluid-acoustic interactions in self-sustained oscillations in turbulent cavity flows fluid-dynamic oscillations. Physics of Fluids Vol.21 No.10 2009.
15. Kaneko K, Matsumoto S, Yamamoto T. Observation of noise of fan with obstacle for electric components. FAN2018; Darmstadt, April 18-20, 2018.
16. Darwish M.S., Moukalled F. Normalized variable and space formulation methodology for high-resolution schemes. Numerical Heat Transfer, Part B Vol.26 1994.p. 79–96.
17. Tsuji Y. Experimental technique to reveal the universality turbulence, Nagare Vol.37 2018. p.245-254
18. Kaneko K, Yamamoto T. Predicting cooling fan noise of electric motor using compressible large eddy simulation. AJK2019; San Francisco, July 28 – August 1, 2019.